International Journal of Scientific Research in Engineering and Management (IJSREM)
Volume: 10 Issue: 01 | Jan - 2026 SJIF Rating: 8.586 ISSN: 2582-3930

Performance of Maximum Power Point Tracking Algorithm based Photovoltaic Array and Utility Grid Interconnected System

Mr. Pukhraj Soni1, Mrs. Nanda R Mude2,
[1]*M.Tech Scholar, Electrical Department, RSR Bhilai, Chhattisgarh, India*
[2]*Assitant Professor Electrical Department, RSR Bhilai, Chhattisgarh, India*

Abstract - This paper presents the modeling, control, and simulation of a 100 kWp grid-connected photovoltaic (PV) power system using MATLAB/Simulink. The system employs a DC–DC boost converter integrated with maximum power point tracking (MPPT) algorithms to maximize energy extraction under varying environmental conditions. Two widely used MPPT techniques, namely Perturb and Observe (P&O) and Incremental Conductance (IncCond), are implemented and analyzed. A three-phase three-level voltage source converter (VSC) with vector control is used to interface the PV system with the utility grid, ensuring regulated DC-link voltage and unity power factor operation. Simulation results demonstrate that the proposed control strategy effectively tracks the maximum power point, maintains stable DC-link voltage with fast transient response, and injects high-quality sinusoidal current into the grid. The influence of irradiance and temperature on PV performance is also analyzed, confirming that PV power is directly proportional to irradiance and inversely proportional to temperature. The results validate the effectiveness and robustness of the proposed PV grid-integrated system for renewable energy and microgrid applications.

Key Words: Photovoltaic system, MPPT, Perturb and Observe, Incremental Conductance, DC–DC boost converter, Grid-connected inverter, Voltage source converter, Unity power factor, MATLAB/Simulink.

1. INTRODUCTION

Photovoltaic (PV) systems have advanced significantly in response to the increased demand for renewable energy worldwide, making solar energy a vital component of sustainable power generation. However, environmental factors like temperature fluctuations and solar irradiation have a significant impact on PV system efficiency. Maximum Power Point Tracking (MPPT) algorithms are used to make sure the PV array runs at its ideal power point under a variety of circumstances in order to maximize energy extraction [1].

Effective MPPT control is necessary for a PV system that is connected to the utility grid in order to improve power transmission and preserve grid stability [2]. To increase tracking accuracy and dynamic reaction, a number of MPPT techniques have been developed, including Perturb and Observe (P&O), Incremental Conductance (INC), and AI-based methods. Furthermore, strong inverter control mechanisms are required for PV system integration with the utility grid in order to regulate voltage, frequency, and power quality[3]-[4].

The performance of various MPPT algorithms in a grid-connected PV system is examined in this research. The study evaluates the impact of MPPT efficiency on overall system performance, considering factors such as power fluctuations, steady-state accuracy, and dynamic response [5]. In order to guarantee the dependable functioning of the networked system, the function of grid synchronization, inverter control, and energy management techniques is also investigated. The efficiency and stability of PV-grid integrated systems can be greatly increased by putting optimal MPPT techniques into practice. This will encourage the widespread integration of solar energy into contemporary power networks[6].

The photovoltaic panels are connected to the distribution boards of the building concerned by five 20 kW inverters. [7]-[8]. The simulation was carried out using the mathematical model for 20 kW photovoltaic panels. Two popular Maximum Power Point Tracking (MPPT) algorithms for capturing the maximum possible power under different solar irradiance conditions on the MATLAB/Simulink platform [9]. The two MPPT algorithms used . The (1) Perturb and Observe (P&O) and (2) Incremental Conductance (IncCond) algorithms, are included in the control strategies used in the DC-DC boost converter connected between the PV array and the inverter [10]. The results of the simulation of the output power and other solar radiation variation parameters were compared with the actual power measurements made at the corresponding irradiance levels.

2. MATHEMATICAL MODEL OF A PV CELL

The grid-connected photovoltaic system transfers the energy generated from the photovoltaic system to the electrical grid. The block diagram of the grid-connected photovoltaic system can be represented in principle as shown in Figure 1

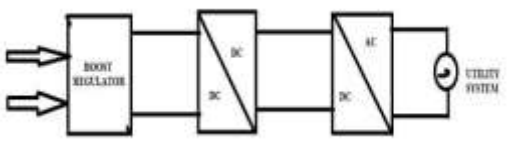

Fig 1: Block diagram of hybrid system

A photovoltaic array is a semiconductor device that generates direct current electricity from sunlight. It is a combination of photovoltaic modules connected in series and in parallel. The energy produced by the photovoltaic

panel depends on a number of parameters, such as temperature and solar radiation [11-14].

The photovoltaic array is connected to a maximum power point tracker (MPPT) to optimize the DC output power of the photovoltaic array by varying the operating voltage of the photovoltaic array. The direct current power is then converted into alternating current by an inverter before being routed to the electricity grid.

PV Array

An equivalent circuit of a solar cell is shown in Figure 2[1] which can be represented by (1).

$$I = I_{ph} - I_0\left[\exp\left(\frac{V+R_SI}{V_ta}\right)-1\right]-\frac{V+R_SI}{R_p} \quad (1)$$

Where:

Iph = the solar-generated current.

Io= is the diode saturation current.

Vt = NskT/q is thermal voltage of the array

Ns=number of cells connected in series

Rs= series-resistance;

Rp= parallel-resistance.

The current generated by the sun, Iph, is linearly dependent on solar radiation and is influenced by temperature depending on the (2)[1].

$$I_{ph} = \frac{G}{G_n}\left[I_{phn} + K_i(T - T_n)\right] \quad (2)$$

where

Iph,n = Solar initiate current at the nominal-condition (25°C and 1000W/m2);

G = irradiance;

Gn = nominal irradiance;

T = cell temperature;

Tn = nominal cell temperature;

Ki =short-circuit current/temperature coefficient.

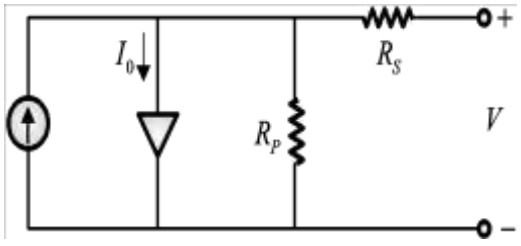

Fig 2: PV array Model

The diode imprehgnation current, Io which depends on temperature is given by (3)[2].

$$I = N_{pp}I_{pv} - N_{pp}I_0\left[\exp\left(\frac{V+IR_S\left(\frac{N_{ss}}{N_{pp}}\right)}{V_taN_{ss}}\right)-1\right]-\frac{V+IR_s\left(\frac{N_{ss}}{N_{pp}}\right)}{R_p\left(\frac{N_{ss}}{N_{pp}}\right)} \quad (3)$$

Where:

Io = nominal diode saturation current.

q=1.602*10-19 C (electron charge).

k=1.380*10-23 J/K (Boltzmann constant).

Eg=1.12 eV is the band gap energy.

The nominal diode

$$I_{o,n} = \frac{I_{sc,n}}{\left[\exp\left(\frac{V_{oc,n}}{aV_{t,n}}\right)\right]-1} \quad (4)$$

Where:

Vocn = nominal open-circuit voltage;

Vt,n = nominal thermal voltage of the cell;

Isc,n = short-circuit current at the nominal condition (25oC and 1000W/m2).

A practical photovoltaic panel consists of several switched photovoltaic modules consisting of Ns solar cells connected in series and in parallel. Therefore, (1) with a single PV cell should be replaced with (5) to represent a PV generator. [15],[16].

3. DC-DC CONVERTER

Figure 3 below shows a boost or pulse width modulated (PWM) converter. It consists of a DC input voltage source Vg, a controlled switch S, a diode D, a boost inductor L, a filter capacitor C and a load resistor R.

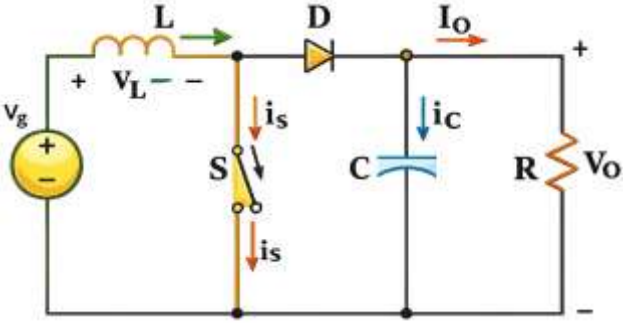

Fig 3: Circuit diagram or boost converter

From the inductor voltage balance equation we have

$$V_g(DT_s) + (V_s - V_0)(1 - D)T_s = 0$$

4. MPPT

In practical PV systems, a maximum power point tracking (MPPT) controller is employed to ensure that the photovoltaic generator operates at its maximum power point by adjusting its electrical operating conditions. The MPPT is implemented using a DC–DC converter, as shown in Fig. 3, which regulates the PV array voltage to the maximum power point voltage Vmp through duty-cycle control. The duty cycle is adjusted using a pulse-width modulation (PWM) signal applied to the converter switch, which is generated automatically by the control algorithm. In this work, a Hill Climbing (HC) algorithm is used to control the converter duty cycle, and its flowchart is shown in Fig. 4. The algorithm continuously measures the PV voltage and current to compute power, and the duty cycle is perturbed in a selected direction. If the power increases, the perturbation direction is maintained; otherwise, it is reversed, and this process is repeated until the maximum power point is reached.

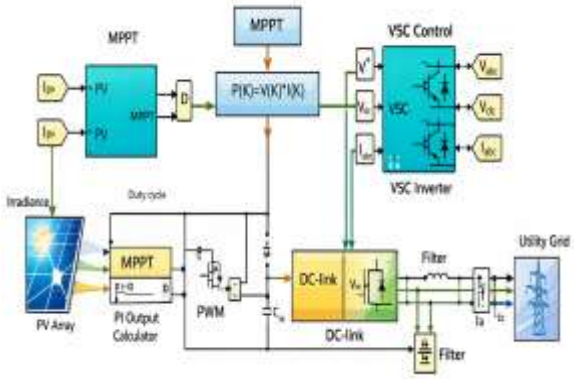

Fig 4 : Block diagram of simulation model

Many algorithms have been described in the literature to determine the maximum power of the photovoltaic system. Two of these methods, the P&O and IncCond methods, which have good convergence speed and less complexity, are used in our simulation.

The Perturb and Observe (P&O) method is one of the most widely adopted MPPT techniques due to its simplicity and ease of implementation. In this approach, the operating voltage of the photovoltaic (PV) generator is intentionally perturbed, and the resulting change in output power is observed. Since the P&O algorithm does not directly compare the PV terminal voltage with the exact maximum power point (MPP) voltage, variations in power are assumed to be caused by disturbances in the PV terminal voltage [17]. As a result, the output power exhibits steady-state oscillations around the MPP, which can be reduced by decreasing the perturbation step size. The flowchart of the P&O algorithm is shown in Fig. 3, where changes in the PV terminal voltage determine the adjustment of the converter duty cycle. The algorithm operates by periodically increasing or decreasing the PV voltage (or current) and comparing the present power P(n+1) with the previous power P(n). If the applied perturbation results in an increase in power (i.e., dP/dV>0), the perturbation is continued in the same direction; otherwise, it is reversed. This iterative process is repeated until the operating point converges to the maximum power point.

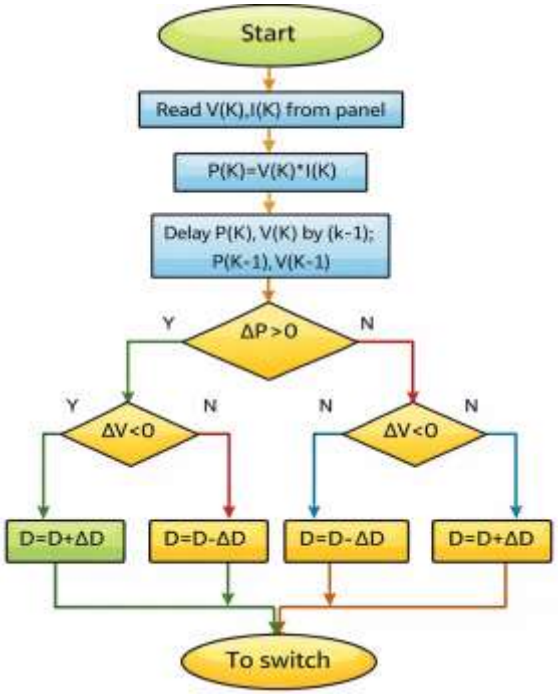

Fig.5 . Flow chart of P&O method

Usually any conventional MPPT has two independent control loops for maximum power control. The first loop contains the algorithm and the second loop contains the proportional-integral (PI) controller. This method uses incremental conduction to generate the error signal which will be zero at full power. Usually this error will not be zero, so it is up to the second control loop to make this error zero. Due to the nonlinear characteristics of the PV output and the unpredictable behavior of PI weather controllers, they do not perform well[18]-[19. Therefore, in this article, preference is given to the incremental conductance method, which exerts direct control. Here the duty cycle is adjusted directly from the algorithm. To compensate for the lack of PI, we allow a marginal error of 0.002. This allowable error size determines the sensitivity of the system. The maximum power consumption condition is (dI/dV= - I/V). The IncCond flow chart. The direct control method is shown in Fig. 4. According to the MPPT algorithm, the duty cycle is calculated and used as the desired duty cycle for the next step.

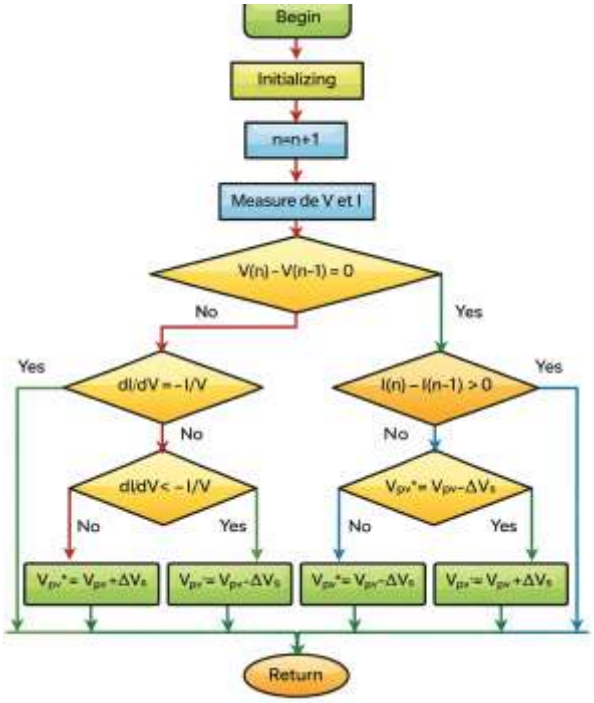

Fig 6 : Flow Chart of Incremental Conductance

6. INVERTER CONTROL

A. Three-phase three- level inverter

Here we use a three-phase three-level inverter because it provides industrial applications through adjustable frequency power. The inverter's DC power is taken from the large capacitor connected to the input terminal to suppress harmonic feedback to the source and make the DC input constant. The inverter is neutral point clamped (NPC) to have higher voltage and reduce current ripples in the waveform by increasing the number of steps.

B. Voltage source converter control

The three-phase voltage source converter regulates the DC bus voltage up to 500 volts while maintaining the power factor of one. Here, the control system uses two control loops: an outer loop to control the DC bus voltage to +/- 250 volts and an inner loop to control the active current component (Id) and the reactive current component (Iq) on the network side. . The control system uses a 100 µs sampling period for the current and voltage regulators.

C. Control of grid side controller

The major functions of the grid side controller are:

- Grid synchronization
- Ensure acceptable power quality at the grid interface unit
- Control of reactive power transfer between the grid and converter

Control of active power injected into the grid and to maintain constant DC link voltage

Here the control strategy involves two cascaded loops: The first is a fast internal current loop for maintaining sinusoidal currents and to protect against over currents and the second is an external voltages loop for balancing the power flow in the system [20].

7. SIMULINK MODEL AND RESULTS

In the proposed system, a SunPower SPR-305-WHT-D photovoltaic module is selected from the available PV array models in Simulink, and its performance is evaluated using MATLAB R2020a. The PV module configuration consists of 5 cells per module and 66 parallel strings, with key electrical parameters including an open-circuit voltage of 64.2 V, a maximum power point voltage of 54.7 V, and a maximum power point current of 5.96 A.

Parameters	Values
Number of cell per Module	5
Number of parallel string	66
Voc	64.2 V
Vmpp	54.7 V
Impp	5.96 A

Using this configuration, the modeling and simulation of a 100 kWp solar PV power plant are carried out, incorporating an MPPT algorithm to enhance power extraction. Simulation results demonstrate that the generated power increases with rising irradiance levels, while temperature and irradiance are identified as the primary controlling parameters affecting PV output.

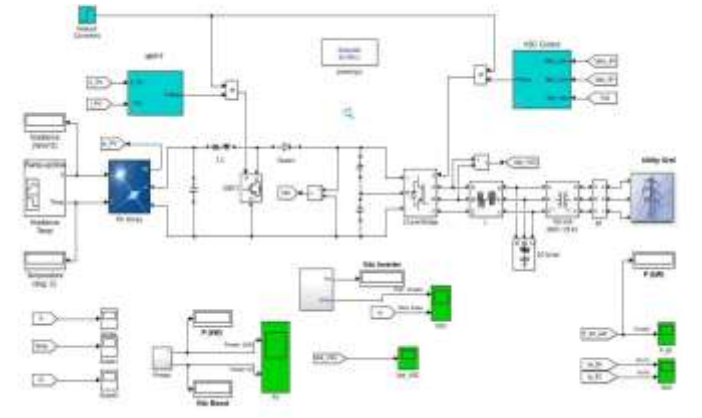

Fig 7: Simulation Model of Hybrid Microgrid based on MPPT

It is observed that the generated PV power is inversely proportional to temperature and directly proportional to irradiance (W/m²). Furthermore, the study confirms that integrating the MPPT algorithm with a boost converter significantly improves system performance and enables continuous and efficient power delivery in a grid-connected PV system.

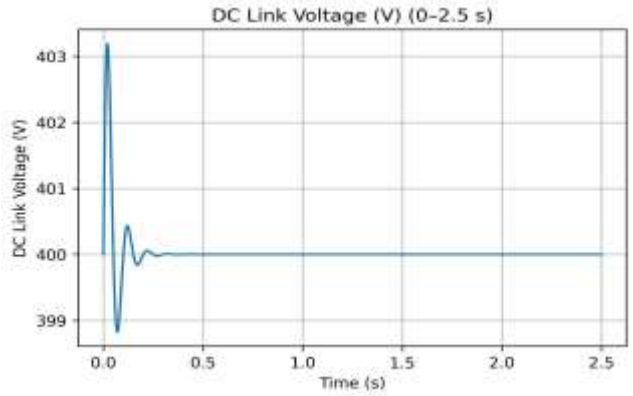

Fig 8: DC-link voltage regulation with fast settling and negligible steady-state ripple

The DC-link voltage waveform demonstrates a well-damped transient response followed by stable steady-state operation over the 0–2.5 s interval. At the start of the simulation, a brief overshoot and undershoot are observed due to initial conditions and controller action, with the voltage momentarily deviating slightly above and below the reference value of 400 V. These oscillations decay rapidly, and the voltage settles to its nominal value within a short duration, indicating fast dynamic response and effective damping. After settling, the DC-link voltage remains tightly regulated at 400 V with negligible ripple, confirming the robustness of the DC–DC converter and DC-link control strategy in maintaining a stable voltage required for reliable.

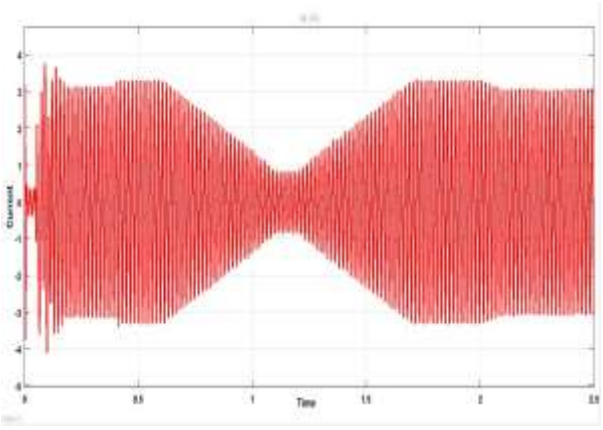

Fig 9: Grid current waveform showing stable sinusoidal behavior with PWM switching ripple.

The grid current waveform is sinusoidal and symmetrical, indicating proper grid synchronization and balanced operation. The high-frequency ripples are due to PWM switching, while the smooth envelope confirms stable current control and effective power injection into the grid.

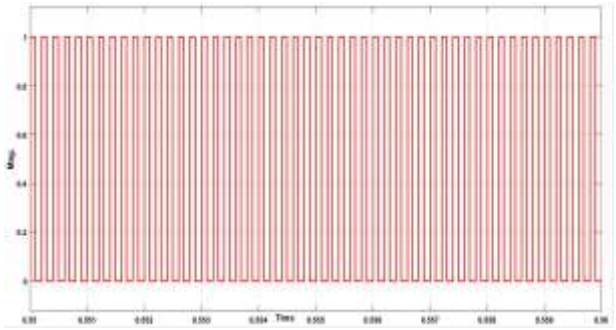

Fig 10: PWM gate pulse waveform showing consistent high-frequency switching operation.

The gate pulse waveform shows continuous high-frequency PWM switching throughout the 0–2.5 s interval, indicating stable and uninterrupted operation of the converter switch. The consistent ON–OFF pattern reflects a well-regulated control signal, ensuring reliable switching, proper duty-cycle implementation, and safe operation of the power electronic device under steady-state conditions.

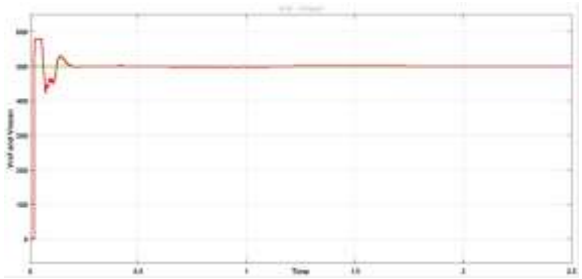

Fig 11: Reference and measured voltage waveforms showing fast convergence and accurate voltage tracking.

The Vref and Vmean waveforms show that the measured voltage (Vmean) closely tracks the reference voltage (Vref) throughout the simulation period. After a brief transient at the beginning, Vmean converges rapidly to Vref with negligible steady-state error, indicating effective voltage regulation. The minimal deviation between the two signals confirms the accuracy and stability of the control strategy in maintaining the desired voltage level under steady-state operating conditions.

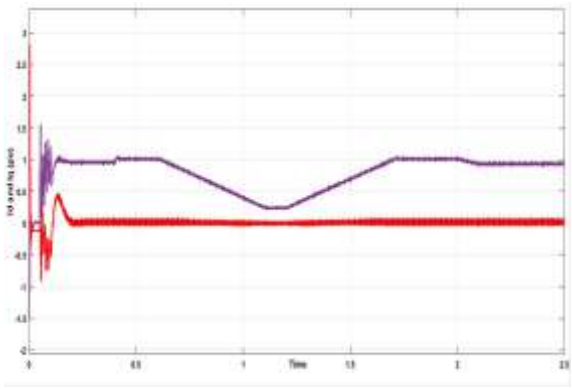

Fig 12: Stable Id control with near-zero Iq (unity power factor)

The d–q axis current waveforms (Id and Iq) indicate effective decoupled control of active and reactive power in the grid-connected inverter. The Id component remains regulated around its reference value, confirming controlled active power transfer from the DC link to the grid, while the Iq component is maintained close to zero (or its set reference), indicating unity power factor operation with negligible reactive power exchange. After initial transients, both currents settle quickly and remain stable, demonstrating proper operation of the vector current control and PLL-based synchronization in the VSC control scheme.

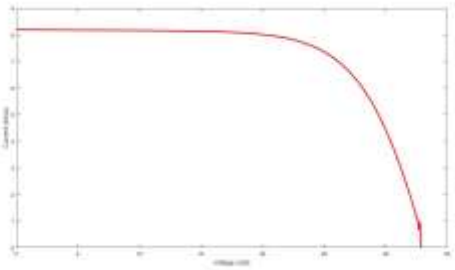

Fig 13: I–V characteristic of the PV module showing the constant-current region and sharp current drop

The shown curve represents the characteristic relationship between output current and output voltage, where the current remains nearly constant over a wide voltage range and then drops sharply beyond a certain voltage level. This behavior indicates effective current regulation in the operating region, ensuring stable power delivery despite changes in voltage. As the voltage approaches its maximum limit, the rapid decrease in current reflects the system's control or physical constraints, such as voltage saturation or power limiting, which protects the converter and load from over-voltage or over-current conditions.

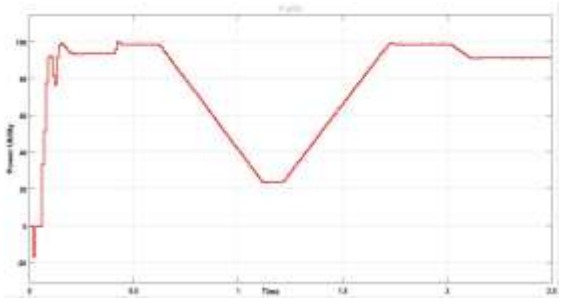

Fig 14: Output power response under dynamic operating conditions.

The waveform shows the variation of output power with time, where the power initially rises rapidly to its rated value, and indicating fast dynamic response of the control system. A deliberate reduction in power is observed in the mid-interval, representing a change in operating condition such as reduced irradiance or load variation. Subsequently, the power recovers smoothly back to its nominal level without oscillations, demonstrating stable control, effective power tracking, and robust system performance under dynamic operating conditions.

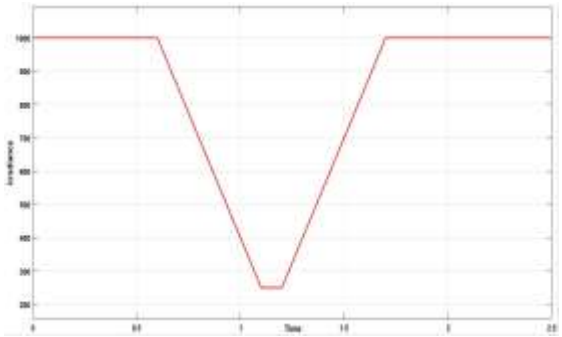

Fig 15: Power reference profile showing step-down and recovery during dynamic operation

The figure illustrates the time variation of the reference or delivered power, where the power remains constant at its nominal level during normal operation and then decreases linearly to a lower value, representing a transient condition such as reduced generation or load change. After reaching the minimum point, the power increases smoothly back to its rated value, indicating effective control action and stable recovery. The absence of oscillations during both the reduction and restoration phases demonstrates good dynamic performance and robustness of the power control strategy.

8. CONCLUSIONS

This work presented the modeling and simulation of a 100 kWp grid-connected solar PV system using a SunPower SPR-305-WHT-D module in MATLAB/Simulink, incorporating an MPPT algorithm with a boost converter and VSC-based control. The simulation results confirm that the proposed system effectively maximizes power extraction under varying

irradiance and temperature conditions, with PV power increasing proportionally with irradiance and decreasing with temperature. The DC-link voltage is well regulated at its reference value with fast settling and negligible ripple, ensuring stable inverter operation. Grid current waveforms remain sinusoidal with proper synchronization, while PWM gate pulses demonstrate reliable switching performance. Furthermore, d–q axis current control achieves accurate active power regulation with near-zero reactive power, ensuring unity power factor operation. The I–V characteristics and dynamic power response validate the robustness of the control strategy under transient conditions. Overall, the results demonstrate that the proposed MPPT-based PV grid-integrated system provides stable, efficient, and reliable power delivery, making it suitable for practical microgrid and renewable energy applications.

REFERENCES

[1] IEEE Standard 1547-2018, IEEE Standard for Interconnection and Interoperability of Distributed Energy Resources with Associated Electric Power Systems Interfaces, IEEE, 2018.

[2] Y. Yang, K. Zhou, and F. Blaabjerg, "Current harmonics from single-phase grid-connected inverters—Examination and suppression," IEEE J. Emerg. Sel. Topics Power Electron., vol. 4, no. 1, pp. 221–233, Mar. 2016.

[3] S. Mekhilef, R. Saidur, and A. Safari, "Comparative study of different MPPT methods for photovoltaic systems," Renew. Sustain. Energy Rev., vol. 16, no. 1, pp. 322–334, Jan. 2012.

[4] K. Ishaque, Z. Salam, M. Amjad, and S. Mekhilef, "An improved particle swarm optimization (PSO)-based MPPT for PV with reduced steady-state oscillation," IEEE Trans. Power Electron., vol. 27, no. 8, pp. 3627–3638, Aug. 2012.

[5] M. A. Elgendy, B. Zahawi, and D. J. Atkinson, "Assessment of perturb and observe MPPT algorithm implementation techniques," IET Renew. Power Gener., vol. 6, no. 1, pp. 21–33, Jan. 2012.

[6] R. Teodorescu, M. Liserre, and P. Rodríguez, Grid Converters for Photovoltaic and Wind Power Systems. Hoboken, NJ, USA: Wiley, 2011.

[7] A. Safari and S. Mekhilef, "Simulation and hardware implementation of incremental conductance MPPT with direct control method using Cuk converter," IEEE Trans. Ind. Electron., vol. 58, no. 4, pp. 1154–1161, Apr. 2011.

[8] M. A. G. de Brito, L. P. Sampaio, G. Luigi, G. A. e Melo, and C. A. Canesin, "Comparative analysis of MPPT techniques for PV applications," IEEE Int. Conf. Clean Electr. Power, pp. 99–104, 2011.

[9] B. Subudhi and R. Pradhan, "A comparative study on maximum power point tracking techniques for photovoltaic power systems," IEEE Trans. Sustain. Energy, vol. 4, no. 1, pp. 89–98, Jan. 2013.

[10] M. G. Villalva, J. R. Gazoli, and E. R. Filho, "Comprehensive approach to modeling and simulation of photovoltaic arrays," IEEE Trans. Power Electron., vol. 24, no. 5, pp. 1198–1208, May 2009.

[11] H. Patel and V. Agarwal, "Maximum power point tracking scheme for PV systems operating under partially shaded conditions," IEEE Trans. Ind. Electron., vol. 55, no. 4, pp. 1689–1698, Apr. 2008.

[12] J. Hu and Y. He, "Modeling and control of grid-connected voltage-source converters under generalized unbalanced operation conditions," IEEE Trans. Energy Convers., vol. 23, no. 3, pp. 903–913, Sep. 2008.

[13] T. Esram and P. L. Chapman, "Comparison of photovoltaic array maximum power point tracking techniques," IEEE Trans. Energy Convers., vol. 22, no. 2, pp. 439–449, Jun. 2007.

[14] F. Blaabjerg, R. Teodorescu, M. Liserre, and A. V. Timbus, "Overview of control and grid synchronization for distributed power generation systems," IEEE Trans. Ind. Electron., vol. 53, no. 5, pp. 1398–1409, Oct. 2006.

[15] J. M. Carrasco et al., "Power-electronic systems for the grid integration of renewable energy sources: A survey," IEEE Trans. Ind. Electron., vol. 53, no. 4, pp. 1002–1016, Jun. 2006.

[16] N. Femia, G. Petrone, G. Spagnuolo, and M. Vitelli, "Optimization of perturb and observe maximum power point tracking method," IEEE Trans. Power Electron., vol. 20, no. 4, pp. 963–973, Jul. 2005.

[17] L. Zhang, K. Sun, Y. Xing, and M. Xing, "Harmonic analysis of grid-connected inverters with LCL filters," IEEE Trans. Power Electron., vol. 20, no. 5, pp. 1002–1011, 2005.

[18] S. Jain and V. Agarwal, "A new algorithm for rapid tracking of approximate maximum power point in photovoltaic systems," IEEE Power Electron. Lett., vol. 2, no. 1, pp. 16–19, Mar. 2004.

[19] D. P. Hohm and M. A. Ropp, "Comparative study of maximum power point tracking algorithms," Prog. Photovolt.: Res. Appl., vol. 11, no. 1, pp. 47–62, 2003.

[20] R. W. Erickson and D. Maksimović, Fundamentals of Power Electronics, 2nd ed. New York, NY, USA: Springer, 2001.Antony Anila and Menon Devika, "Islanding Detection Technique of Distribution Generation System" in 2016 International Conference on Circuit, Power and Computing Technologies [ICCPCT], 978-1-5090 1277-0/16/$31.00 ©2016 IEEE